NUMERICAL INVESTIGATION ON THE INFLUENCE OF THE UPSTREAM FLOW CONDITION ON THE SIGNAL OF THE AIR FLOW METER SENSOR OF A BMW PASSENGER CAR

by

Zoltán KÓRIK
/D6KZEV/

Submitted to the
Department of Fluid Mechanics of the
Budapest University of Technology and Economics
in partial fulfillment of the requirements for the degree of
Master of Science in Mechanical Engineering Modelling

May, 2011

Project Report in Major Project /BMEGEÁTMWD1/

Supervisor:
Jenő Miklós SUDA, PhD assistant professor

Evaluation Team Members, advisors:
Viktor SZENTE, PhD research assistant
László NAGY, assistant lecturer

Department of Fluid Mechanics
Faculty of Mechanical Engineering
Budapest University of Technology and Economics

ASSIGNMENT

MSc MAJOR PROJECT (BMEGEÁTMWD1)

Title:	**Numerical investigation on the influence of the upstream flow condition on the signal of the air flow meter sensor of a BMW passenger car**
Author's name (code):	**Zoltán KÓRIK (D6KZEV)**
Curriculum :	MSc in Mechanical Engineering Modelling / Fluid Mechanics
Supervisor's name, title:	**Jenő Miklós SUDA, PhD, assistant professor**
Affiliation:	Department of Fluid Mechanics / BME
Assistant supervisor's name, title:	**-**
Affiliation:	-

Description / tasks of the project:

In course of the project the upstream air flow condition in the air intake unit and its influence on the MAF signal is to be analysed numerically. Air intake unit of a car usually consists of several elements that may gain influence on the flow condition upstream to the air flow meter (AFM). These elements are e.g. the inlet cone, tubing, filter housing with air filter element and connection piece or guide vanes in the filter housing upstream of the air flow meter unit. The flow condition upstream of the sensor may gain influence on the output voltage signal that is proportional to the mass flow rate. Deviation of the signal due to the upstream flow condition is crucial while the AFM is used (in connection with lambda sensor signal and butterfly valve position signal) to regulate fuel-injection through engine control system (Motronic) to fulfil the strict requirements of the exhaust-gas. Wrong or modified AFM output signal due to the modified upstream flow condition can cause shift between the real and the measured air mass flow rate, hence the digital motor electronic (DME) system may regulate based on wrong signal.

1. 3D geometrical modelling (build up the 3D geometry, meshing) of the elements of the air intake unit and AFM for various elements (original factory intake unit and special filter housing and connection pieces, inlet cones)
2. Run numerical simulation with parameter study, investigate the effect of grid resolution
3. Evaluate the numerical results (if possible - compare to measured data)
4. Make suggestions: for the optimum set-up and for signal correction for the various versions
5. Discussion of the simulation results

Handed out / Deadline: **7th of February 2011. / 13th of May 2011.**

Budapest, 7th of February 2011.

…….
Head of Department

Received by:

The undersigned declares that all prerequisite subjects of the Major Project have been fully accomplished. Otherwise, the present assignment for the Final Project is to be considered invalid. Signed in Budapest, on the 7th of February 2011.

…….
Student

Budapest University of Technology and Economics
Faculty of Mechanical Engineering
Department of Fluid Mechanics

Hungary, 1111 Budapest, Bertalan L. u. 4-6.
Telefon: (36-1) 463-4072 Fax: (36-1) 463-3464
http://www.ara.bme.hu

DECLARATION

Full Name (as in ID):	Zoltán KÓRIK
Neptun Code:	D6KZEV
University:	Budapest University of Technology and Economics
Faculty:	Faculty of Mechanical Engineering
Department:	Department of Fluid Mechanics
Major/Minor:	MSc in Mechanical Engineering Modelling Fluid Mechanics major / Solid Mechanics minor
Project Report Title:	Numerical investigation on the influence of the upstream flow condition on the signal of the air flow meter sensor of a BMW passenger car
Academic year of submission:	2010 / 2011 - II.

I, the undersigned, hereby declare that the Project Report submitted for assessment and defence, exclusively contains the results of my own work assisted by my supervisor. Further to it, it is also stated that all other results taken from the technical literature or other sources are clearly identified and referred to according to copyright (footnotes/references are chapter and verse, and placed appropriately).
I accept that the scientific results presented in my Project Report can be utilised by the Department of the supervisor for further research or teaching purposes.

Budapest, 13 May, 2011

_____

(Signature)

FOR YOUR INFORMATION

The submitted Project Report in written and in electronic format can be found in the Library of the Department of Fluid Mechanics at the Budapest University of Technology and Economics. Address: H-1111 Budapest, Bertalan L. 4-6. „Ae" building of the BME.

ACKNOWLEDGEMENT

It is a pleasure to thank those who made this project possible with their guidance and support. I offer my regards to my supervisor Jenő Miklós SUDA and all the members of the Department of Fluid Mechanics who helped me at the evaluation team meetings. I would like to thank the cooperation of Marcell BORIÁN who provided the measurement data.

Zoltán KÓRIK

ABSTRACT

In this project the effect of the presence of a funnel on the upstream flow conditions of an air flow meter (AFM) – which is used in a passenger car – were investigated by numerical simulations. The main parts of the air intake system were modelled in 3D with SolidWorks. The important geometry features were kept, the unimportant ones were neglected during the geometry reconstruction.
Meshes were generated for six different cases (three flap angle position with and without funnel). The boundary conditions of the simulation based on measurements – carried out by Marcell BORIÁN.
The measurements showed that the case with small flap angle does not occur in real operation (even at idle engine operation the flap angle is higher), therefore four cases were simulated. The static pressure results of the measurement and the simulation were compared.
One of the two different flap angle cases gave similar results, but the difference of the other results were significant at the outflow of the AFM. The resulting flow fields showed significant difference in the topology of the flow upstream the flap.
Further investigations are planned to be carried out in Final Project.

KIVONAT

Ebben a projectben egy személyautóban használt légmennyiségmérő rááramlás képe és annak hatása került vizsgálatra egy beszívótölcsér jelenlétének függvényében numerikus szimuláció segítségével. A légbeszívórendszer főbb elemeinek modellje SolidWorks-szel készült 3D-ben, figyelembe véve a néhány fontosabb részleteket is, de az áramlás szempontjából elhanyagolható geometriai részletek egyszerűsítésével.
Öszesen hat különböző háló készült (három torlólap szögpozíció, beszívótölcsérrel és beszívőtölcsér nélkül). A szimulációk peremfeltételeinek beállítása a BORIÁN Marcell által elvégzett mérések alapján történt.
A mérési eredmények kimutatták, hogy valós körülmények között a legkisebb szögpozíció nem fordul elő (alapjáraton is nagyobb a nyitási szög), ezért négy eset lett lefuttatva. A szimulációs és a mérési adatok közül a statikus nyomásértékek lettek összehasonlítva.
Az egyik szögpozíció esetén a szimulációk és a mérési eredmények jól egyeztek, azonban a másik szögpozíció esetén a légmennyiségmérő kilépő keresztmetszeténél mérhető nyomásértékek jelentősen eltértek. A beszívótölcsérrel illetve beszívótölcsér nélkül kapott rááramlások áramképei jelentősen eltértek.
A Final Project tárgy keretein belül további vizsgálatok készülnek majd.

CONTENTS

NOMENCLATURE

A	area [m^2]
k	turbulent kinetic energy [$m^2 \cdot s^{-2}$]
$\dot{m}$	mass flow rate [$kg \cdot s^{-1}$]
N	number of cells [-]
p	static pressure [$N \cdot m^{-2}$]
V	volume [m^3]
x	x coordinate [m]
y	y coordinate [m]
z	z coordinate [m]

GREEK INDEX

α	flap angle [º]
β	reference angle [º]
λ	air ratio [-]
μ	dynamic viscosity [$kg \cdot m^{-1} \cdot s^{-1}$]
ρ	density [$kg \cdot m^{-3}$]
ω	specific dissipation rate [s^{-1}]

1 INTRODUCTION

1.1 Aim of the project

The aim of the project is to investigate the influence of the upstream flow condition on the signal of an AFM (air flow meter) of a passenger car. The AFM is used to measure the actual intake mass flow rate of the engine. The upstream elements to the AFM are designed to allow low pressure loss and proper, streamlined air flow distribution upstream of the flow rate measuring cross section of the AFM. At the AFM inlet there is a funnel that's role is to minimize the losses to the Borda-Carnot type flow section. Since the existence of the funnel has big influence on the flow field in the top of the filter house and in the AFM before the flap, it may happen that the AFM gives a different signal with same flow rate depending on that there is the funnel or not. So if the signal is different than the one that corresponds to the real mass flow rate value, the air-fuel mixture will not be optimal. This is crucial because the amount of fuel not only influences the consumption and the performance (see **Figure 1.1**), but the emission as well. (λ = input air amount / air amount required in theory)

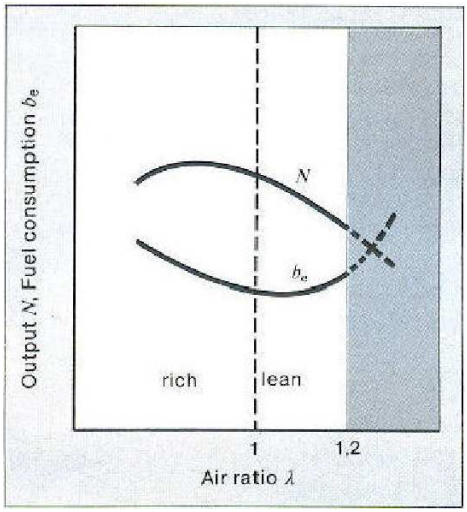

Figure 1.1 - Fuel consumption and output depending on the air ratio [1]

To know the optimal amount of fuel that has to be injected into the cylinders – to have proper operation, a few parameters one to be measured:

- The position of the throttle pedal – e.g. we want to accelerate
- The current rotational speed (rpm) of the engine
- The temperature of the engine
- The amount of air which is drawn by the engine

All these main parameters (and others) are measured and the signals are forwarded to the engine control unit (ECU).

(Remark: the abbreviation ECU in vehicle industry often stands for electric control unit, which can be responsible for different things, e.g. the control unit of air brake systems on trucks and buses. But since a few decades the engine control unit is realized with an electronic system – in the first half of the 20th century mostly mechanical and pneumatic solutions existed – it is an electric control unit. Further on in this document the ECU will refer to the engine control unit.)

Since the combustion is a chemical process, we have to know the mass flow rate of the air drawn by the engine. This can be measured by different devices, which work due to different principles.

In this document the following type AFM and the connecting devices will be introduced and investigated.

1.2 Parts of the system

Device list (only the important parts for the present investigation)

Numbers on **Figure 1.2**

1	Air Flow Meter	BOSCH 028 0 2020 203
2	Sealing frame	13711705064 (number 9 on **Figure 1.3**)
4	Rubber boot	13711709754*

Numbers on **Figure 1.3**

1	Intake muffler	13711709756
2	Air filter element	13721715881 (MANN filter element)
10	Funnel	13711709769
12	Intake tube	13711727097

* Another type of rubber boot (see in Appendix, **Figure A.5**) was used during the measurement instead of the original rubber boot (13711721431), because the original one evolves to oval cross section towards the intake manifold of the engine and it is difficult to connect to the orifice plate measurement system.

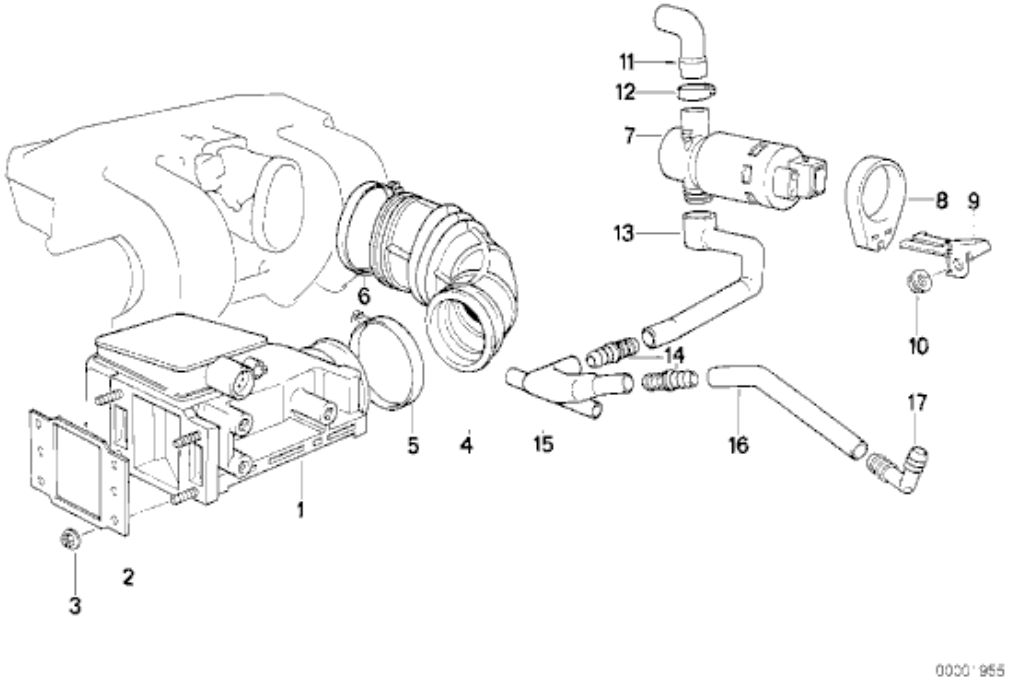

Figure 1.2 – Parts from the filter house to the engine [2]

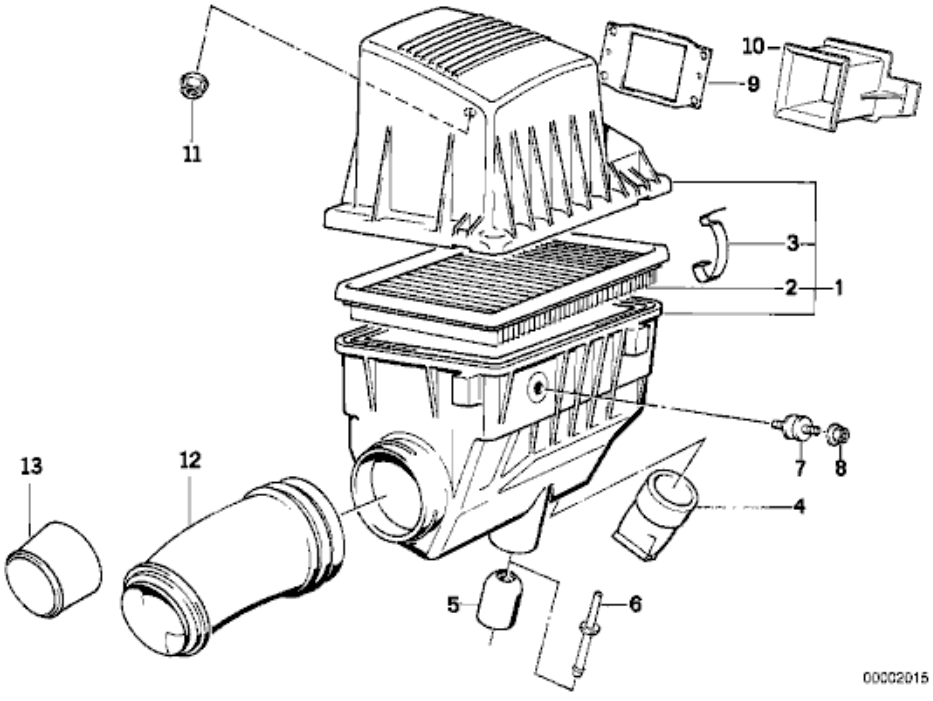

Figure 1.3 – Parts from the inlet to the AFM [2]

The air comes from the headlight surroundings body through an intake tube (12), and then it enters in the filter house (intake muffler) (1). Inside the filter house there is a filter (2) and a funnel (10). Between the AFM and the filter house there is a sealing

frame (9). After the filter house the air enters into the AFM, and then it goes through a rubber boot which connects this system to the intake manifold of the engine. This tube is the last element of the investigated model. The picture below (**Figure 1.4**) shows the system in the car.

Figure 1.4 – The system in the car

1.3 The working principle of the AFM [1]

“The principle is based on the measurement of the force emanating from the stream of air drawn in by the engine. This force has to counteract the opposing force of a return spring acting upon the air-flow sensor flap. The flap is deflected in such a manner that, together with the profile of the measurement duct, the free cross-section increases along with the rise in the quantity of air passing through it.” The free cross-section depends on the position of the flap, so the position of the flap indicates the air flow rate. The position is measured by a potentiometer.

Since the volumetric efficiency of the cylinders drops for the same throttle-valve position as the temperature increases the air temperature is measured too. It allows us to measure the mass flow rate, since density of air can be calculated based on the temperature sensor.

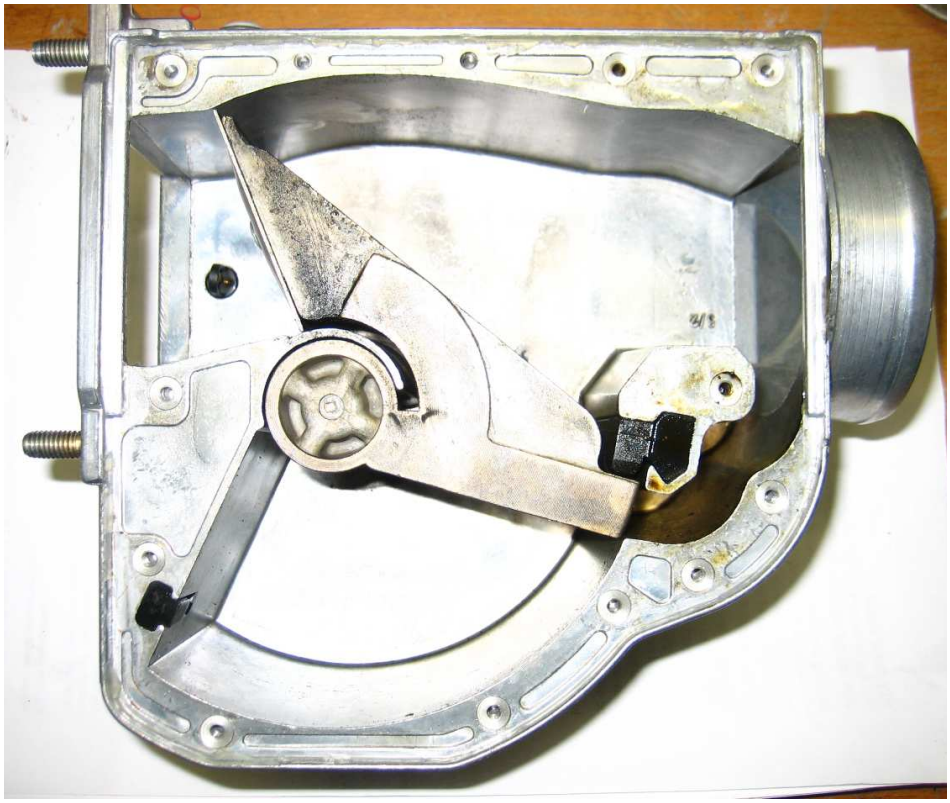

Figure 1.5 – The AFM – flap is closed

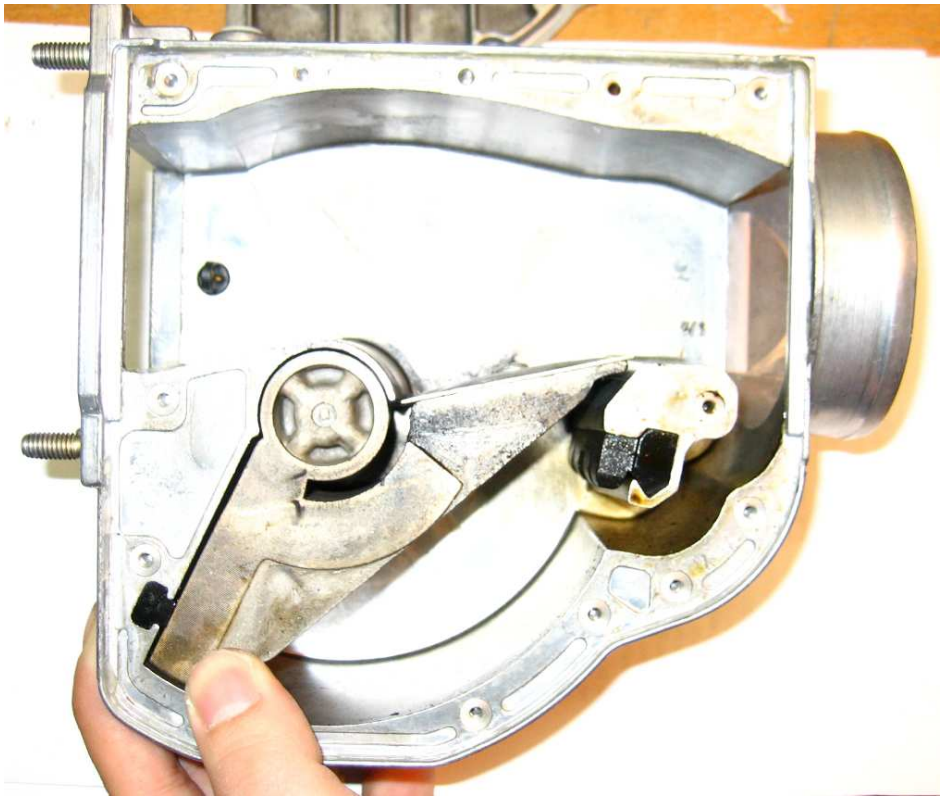

Figure 1.6 – The AFM – flap is fully opened

2 CREATING THE GEOMETRY

2.1 Modeling method

The geometry was reconstructed with SolidWorks. Most of the dimensions (distances, diameters, curvatures, angles, etc.) were measured for all elements, while some dimensions were only possible to be estimated with the help of the others due to the fact that some of them were impossible to access without special measuring tools. Some of less important data were assumed to be constant (e. g. the thickness of the wall of the plastic components).

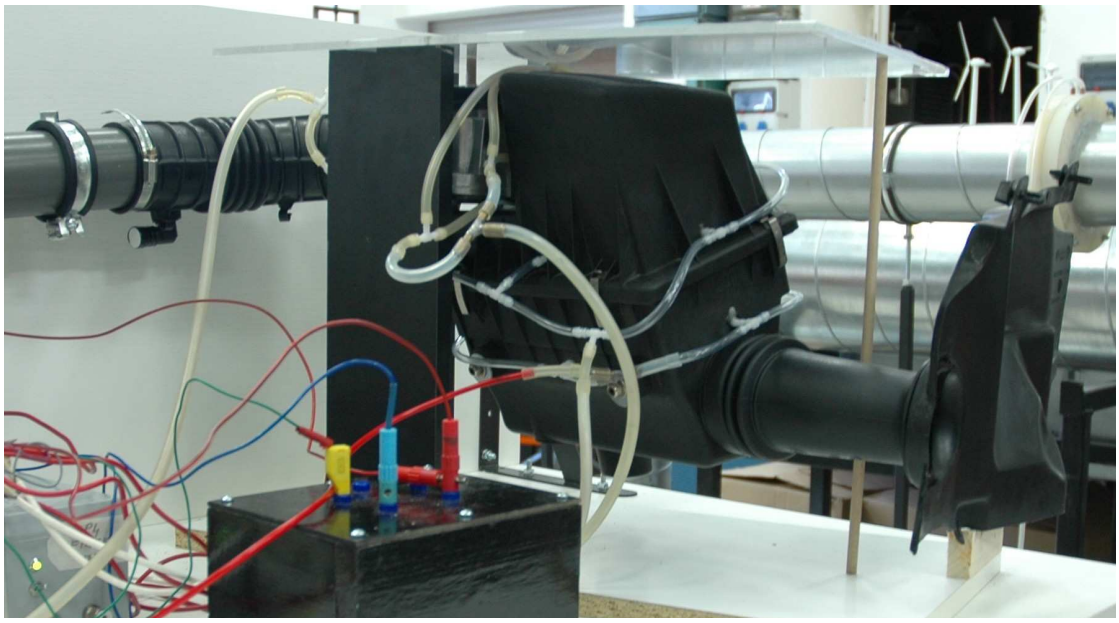

Figure 2.1 – The measurement set-up

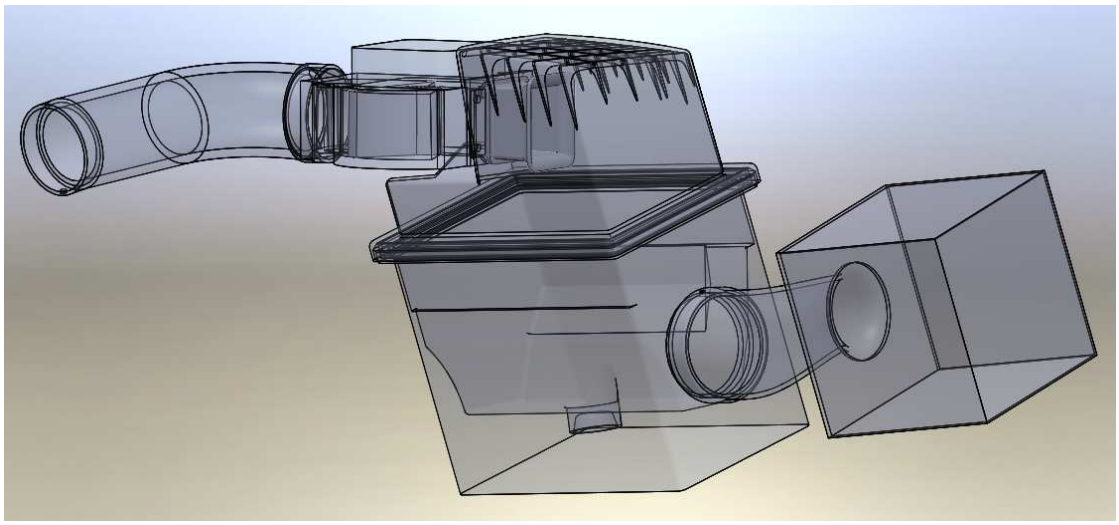

Figure 2.2 – The modelled geometry

2.2 Simplifications

Since only the inner volumes are important in this problem, the outer surfaces of the parts were modeled only roughly in most cases. Therefore different features such like the ribs on the top of the filter house on the outer surface were not modeled at all.

The following geometry details were not modeled:

- The spur of the funnel which is responsible for fastening it to the top of the filter house and the connecting geometry in the filter house was neglected too.
- The fastening screws which connect the AFM to the filter house.
- The sealing frame was not modeled, but its thickness was taken into account to the top of filter house.
- The filament of the temperature sensor was neglected, only the body of it "floats" in the AFM.
- Fillets with radius below 0.5 mm were considered as sharp edges.
- The head profiles of the screws in the flap were neglected.
- The bottom and top geometry of the back of the flap were simplified.
- The bumper components in the AFM were considered as simple bars and they were merged to the main body.
- The accordion-like features of the intake tube and the rubber boot were neglected, their inner surfaces were considered as smooth surfaces.

2.3 Kept details

Some small features were modeled, which are supposed to have great influence on the mesh cell number, but on the flow field as well.

- The ribs on the top of the inner surface of the filter house. (**Figure 2.3**) (These ribs are mainly used to strengthen the plastic structure, but effect the inner flow field near the walls, too.)
- The face profile of the flap except the head profiles of the screws. (**Figure 2.4**)
- The temperature sensor and the sensor protector element. (**Figure 2.4**)

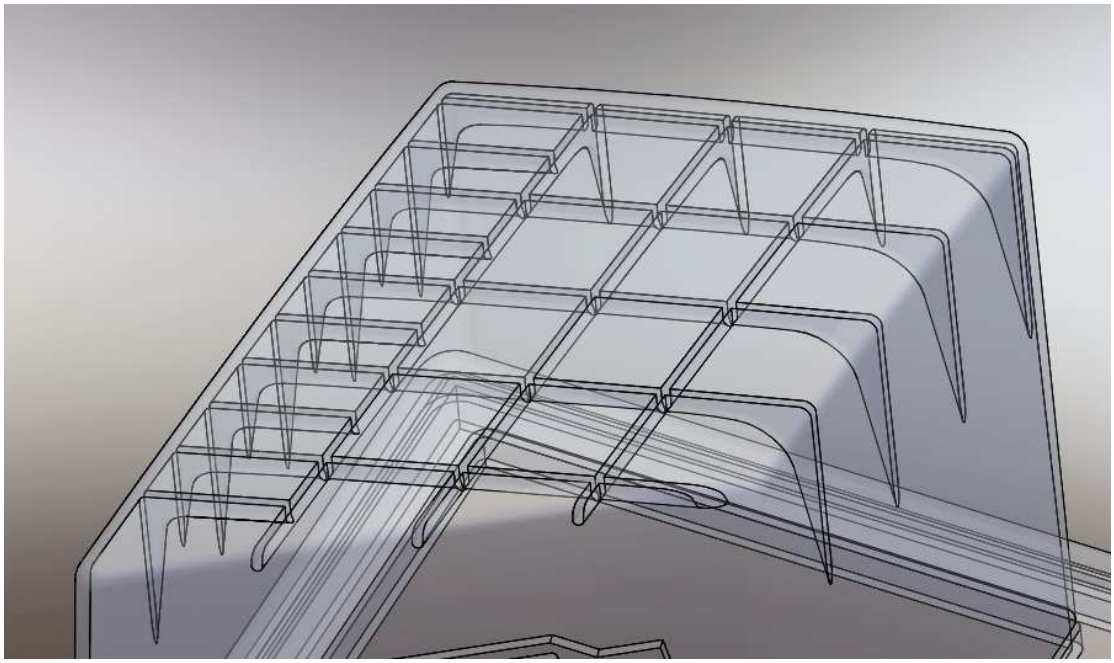

Figure 2.3 – The ribs on the inner surface of the upper filter house

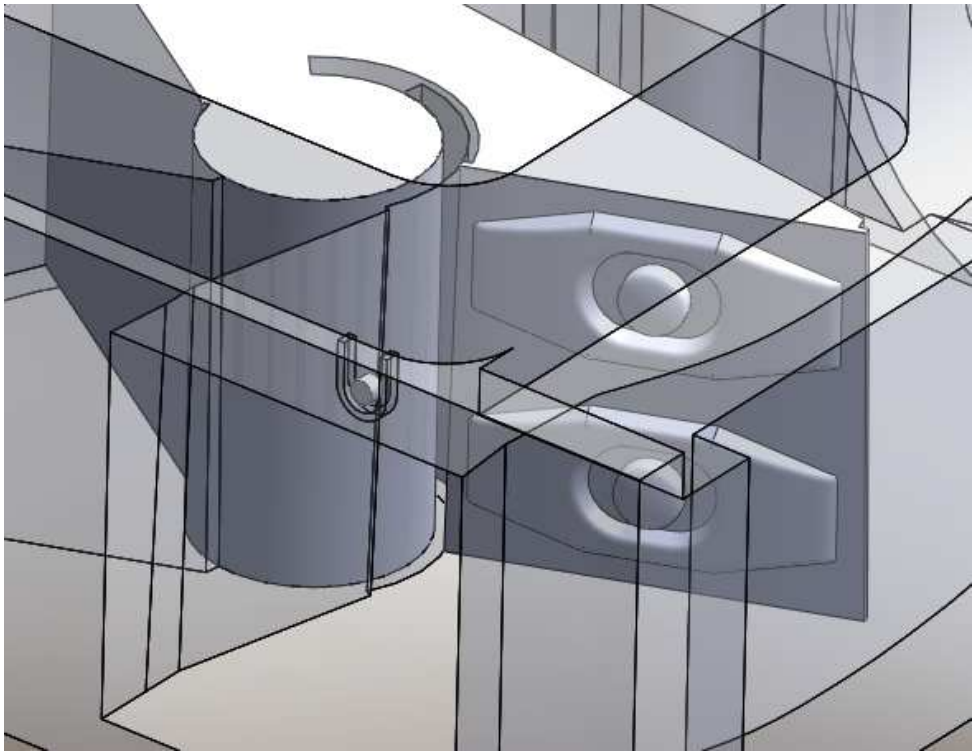

Figure 2.4 – The front face of the flap and the temperature sensor (the AFM house is translucent)

2.4 Modeling of the inlet

The air comes from the headlight surroundings to the intake tube. The inner covering of the left headlight has a circular opening. In this opening sits the intake tube. The real shape of the inner covering was neglected, a single plane was used as an inlet wall surrounding the circular inlet. The intake tube is connected directly to this plane which is parallel to the inlet cross section of the tube. To take this wall into account, a simple box what added to the domain, which has this wall and the other sides are the free inlet surfaces. The size of the box was minimized to use as low cell number as possible.

2.5 The assembly

The model was created part by part. The parts were assembled with different mates, to have the proper connections. The first part in the assembly was the AFM house. The reason for this is that the coordinate system should be aligned to this part to have a well defined flow direction (z axis). Therefore, the z axis serves as the mean flow direction in the AFM inlet cross section that has a rectangular shape. So it makes the definition of different cross sections easier, where the simulation results are to be plotted and analysed.

Figure 2.5 shows the inlet cross section with dimensions.

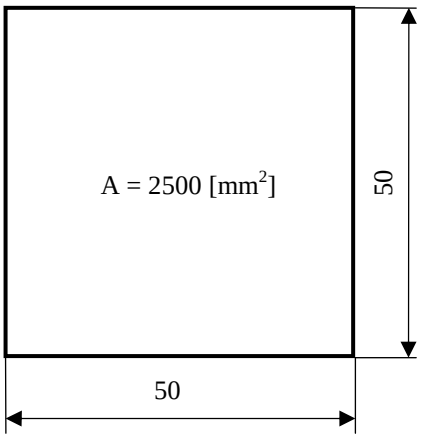

Figure 2.5 – The inlet cross section of the AFM

2.6 The CAD geometry

Figure 2.6 shows the full geometry of the model, **Figure 2.7** and **Figure 2.8** focus on the AFM and its surroundings. The filter is not modeled yet in the present case, it will be handled as a porous zone for the further investigations.

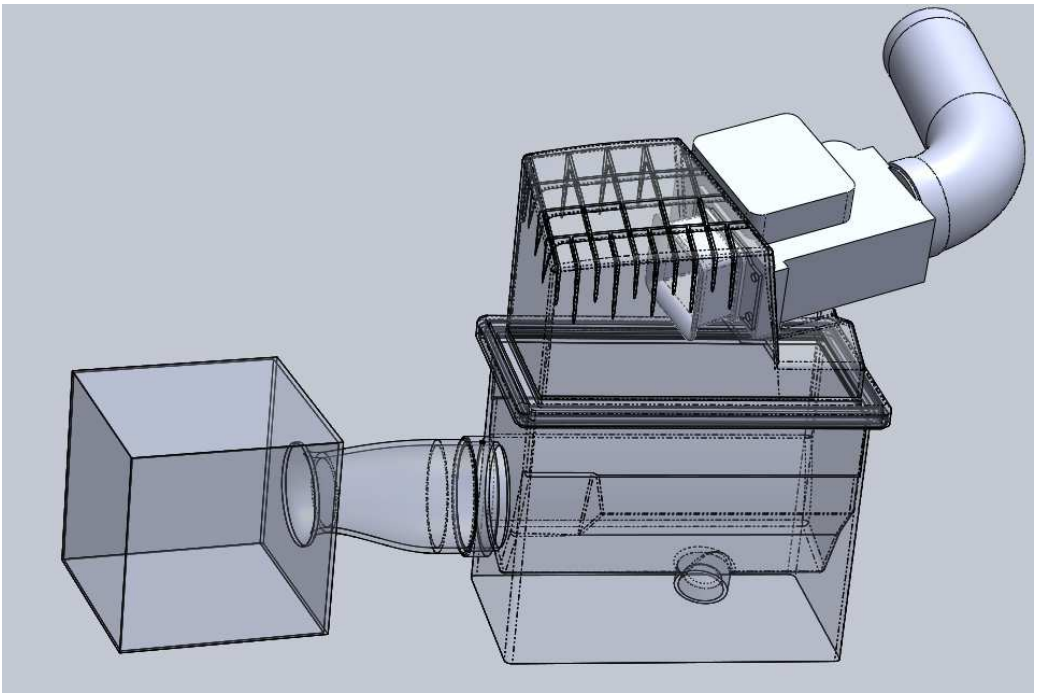

Figure 2.6 – The whole intake system

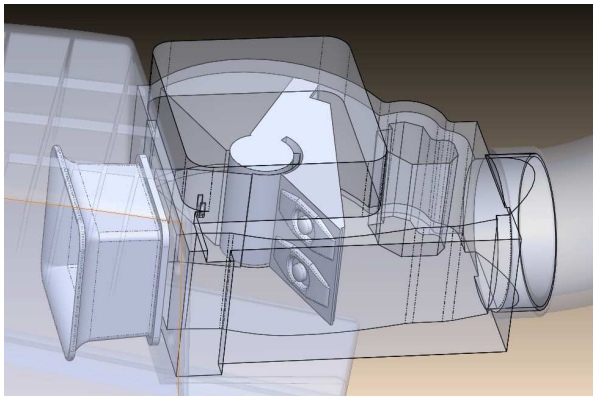

Figure 2.7 – The AFM and the funnel

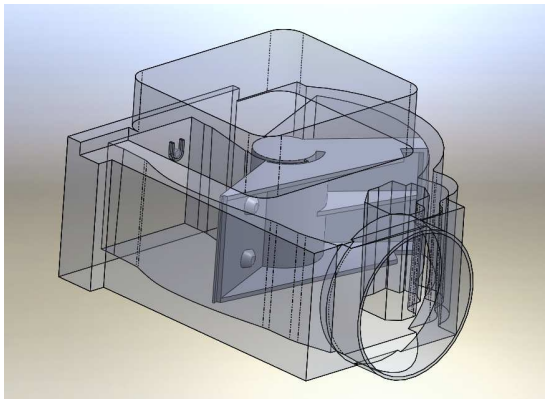

Figure 2.8 – The AFM

2.7 Planned cases

Figure 2.4, 2.5 and 2.6 shows the flap with 3 different opening angles. At rest, the flap is in fully closed (0º angle) position. After starting the engine the idle state flap angle is 40º degrees and at full throttle the maximum allowed opening angle is 99º degrees.

Simulations were planned to carry out with 3 different flap angles.

- with a very small gap between the flap and the wall (**Figure 2.9**)
- with a medium gap between the flap and the wall (**Figure 2.10**)
- with a large gap between the flap and the wall (**Figure 2.11**)

Further on the following notations will be used for different cases.

A0 Small gap (Figure 2.9) without funnel

A1 Small gap (Figure 2.9) with funnel

B0 Medium gap (Figure 2.10) without funnel

B1 Medium gap (Figure 2.10) with funnel

C0 Large gap (Figure 2.11) without funnel

C1 Large gap (Figure 2.11) with funnel

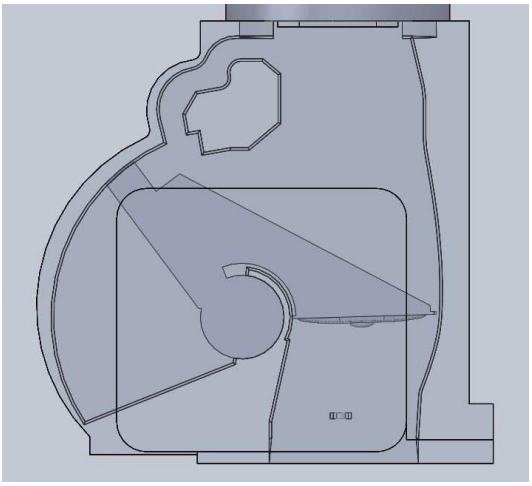

Figure 2.9 – Small gap (A case)

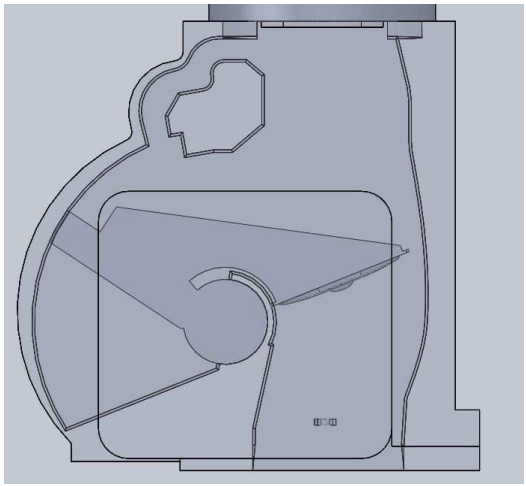

Figure 2.10 – Medium gap (B case)

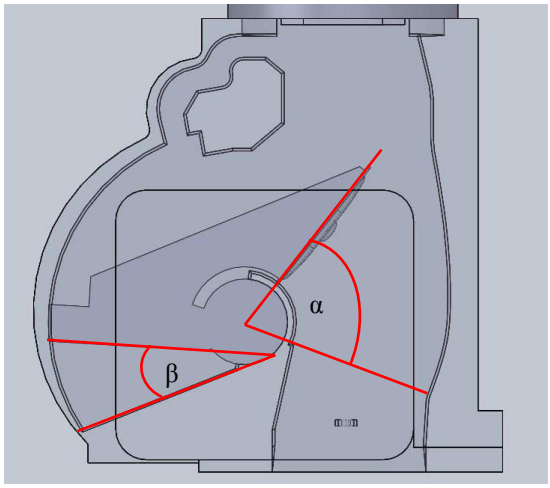

Figure 2.11 – Large gap (C case) – with reference and flap angles

All these cases were planned to investigate with the funnel inside and without it.

2.8 Simulated cases

It turned out from the measurement, that at idle RPM the engine draws such an amount of air, which turns the flap already with a quite high angle. This angle is 40º measured from the closed position.

Since in reality the A cases (i.e. $\alpha < 40º$) never occur with proper idle RPM, and due to the fact that the mesh for these cases have high cell number (over 2 million, see **Table 3.1**) these cases for simulation were cancelled, but basic meshes were created for these cases before this fact was realized.

Since the inside geometry of the AFM is complex, it was difficult to choose a reference for flap angle definition. The selected reference was the edge of the damping chamber, which is approached by the flap when it is in fully opened position (see on **Figure 2.11**). The 3 planned angles for this reference was: 25º, 55º and 75º. After matching the real flap angle positions and these reference angles we got **Table 2.1**:

Table 2.1 – Reference and flap angles

Case	Reference angle (β)	Flap angle (α)
A	75º	22º
B	55º	42º
C	25º	72º

So the simulated cases were the cases with flap angle 42º and 72º.

2.9 Planes for plots

To investigate the flow field some planes through the AFM and some near to it needed to be defined. **Table 2.2** (below) shows the constant coordinates and every plane has a number which can be found on **Figure 2.12** and **Figure 2.13**. The red colour shows the coordinate system.

Table 2.2 – Constant coordinates of the cross sections

Number	Name	x	y	z
1	Funnel inlet			44.5
2	Funnel end			4.5
3	AFM inlet			0
4	Temp. s. midpoint - z			-16
5	Flap rotation axis			-49
6	Flap edge - small gap			-50
7	Flap edge - medium gap			-72.1
8	Flap edge - large gap			-99.4
9	Circ. cross section beg.			-148
10	AFM outlet			-168
11	Horizontal 1/4		19.5	
12	Horizontal mid-plane		32	
13	Horizontal 3/4		44.5	
14	Horizontal temp. sens. mid.		51.5	
15	Vertical mid-plane - x	-50		

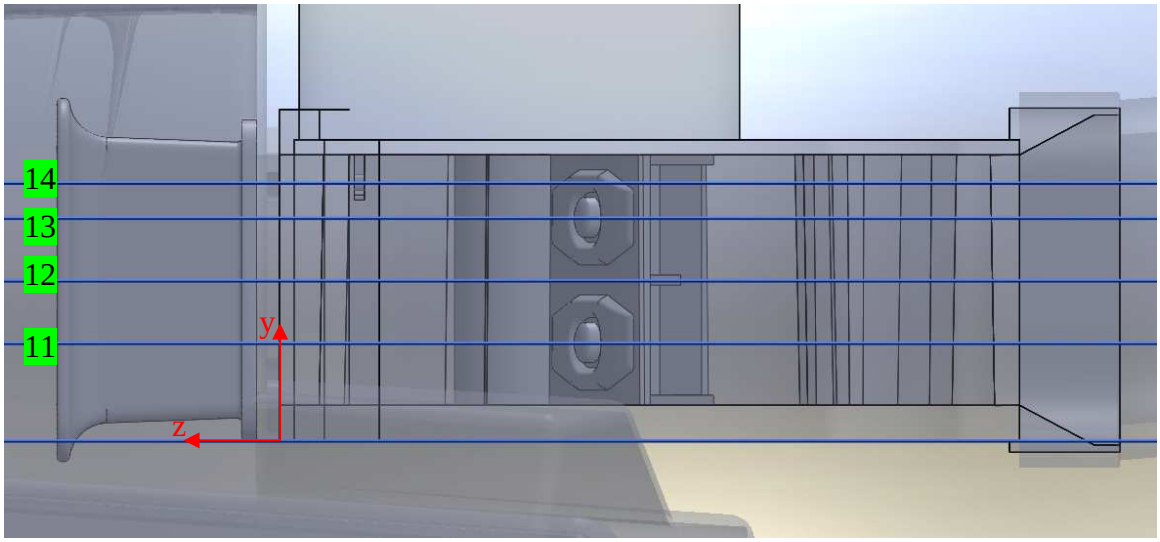

Figure 2.12 – Horizontal planes in the AFM (see Table 2.2 for the numbers)

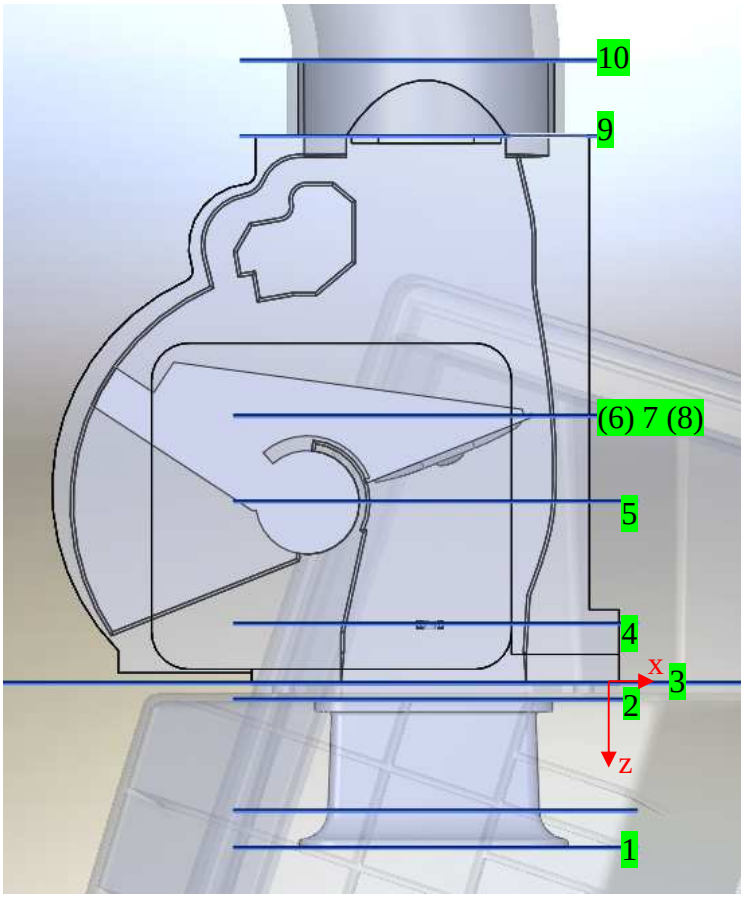

Figure 2.13 – Vertical planes in the AFM (see Table 2.2 for the numbers)

Remark: the 15th plane is not shown on the pictures.
With some of these planes the results can be validated to the measurements.
During the measurement the plane Nr. 9 was measured as AFM outflow cross section.

3 MESHING

3.1 Getting the inner surface geometry

The model was saved in STEP format and was imported to ICEM CFD. To have all the needed curves, surfaces and points the feature “Build Topology” was needed to run. After this the outer surfaces, curves and points were deleted. After this only the inner surfaces remained.

3.2 Assumption

Since the whole geometry is quite large and it has small features which had to be resolved by the mesh, this means a large number of cells. An opportunity to decrease the number of cells significantly is the following.

No filter element is modeled, moreover the whole upstream parts to the filter elements are neglected for the present simulation. Therefore only the top part of the geometry (after the filter) was kept and meshed for all cases.

The filter has a high loss factor in the system, so it can be assumed that the flow just over the filter is quite uniform. This assumption is planned to be checked in the future of course.

3.3 Identification of the surfaces

Most the surfaces were renamed in order to identify them for different reasons. For example: to have some surface which can be monitored to watch the convergence of the solution.

Some surfaces were split in order to control the detail parameters of the mesh. (E.g. the wall of the AFM in front of the edge of the flap)

3.4 The meshing method

The build-up procedure of a structured mesh would be very time consuming and difficult, because a lot of blocks should be generated since the geometry is very complex.

Another option is to build structured mesh on parts which have simple geometry (e.g. the rubber boot) and build unstructured mesh on the others, then connect the meshes together through interfaces. In this method it is crucial to have the same node locations on the connecting interfaces, because if it is not so, then it can result in wrong solution.

The third method which was selected is that to build the whole mesh as unstructured with the “Octree” method, which is very robust. However, this method results with a higher number of cells, but the integrity of the mesh is guaranteed.

3.5 Target number of cells

The target was to have a mesh which has less than 2 million cells, because the number of cells has a great impact on the computational time. But with smaller gap between the flap and the wall the number of cells have to be increased, because the gap has to be resolved properly (at least 5-10 cells in the gap).

3.6 Prism layers

The highest velocity is expected in the gap near the walls, where the flow is deflected to by the flap. To have a good mesh in this region is important, therefore prism layers were build on the vertical walls in front of the flap in all cases and on the front face and on the side of the flap in most cases.

In the case of the smallest gap very little cells (0.15 [mm] height) were applied to resolve the gap properly, but because of this the ratio of the largest and the smallest cell sizes is so large, that a prism layer with constant parameters along the flap would result in a big cell size jump in the originally coarser region. It would be difficult to split the front face of the flap due to its complex geometry, so in the case of the smallest gap prism layer was not build on the flap.

3.7 Final meshes

The number of cells are shown on **Table 3.1**.

Table 3.1

Case	Number of cells (N)
A0	2136000 *
A1	2240000 *
B0	1124465
B1	1256591
C0	608562
C1	819652 **

* Approximate numbers, only initial mesh was created without smoothing operations, due to the cancelled cases.

** With the basic parameters, some disoriented surface cells were created in the ribs (the reason was unknown, the same parameters worked well for all other cases), therefore the parameters of the following was changed (see **Table 3.2**):

Table 3.2

	Max. size		Min. size limit	
Part name	Old	New	Old	New
RIBS	5	3	1	0.5
WALL BETWEEN RIBS	8	5	1	0.8

Furthermore only the simulated case meshes will be detailed.

(An “A” case mesh can be seen in the Appendix, **Figure A.2** and **Figure A.3**)

The mesh parameters are shown on the next page (**Table 3.3** and **Table 3.4**).

Table 3.3 - The mesh parameters in case “C”

Part name	prism	max size	height	height ratio	num layers	tetra size ratio	tetra width	min size limit
AFM		5	0	1.1	0	1.2	0	1
FLAP		5	0	1.1	0	1.2	0	1
FLUID		15						
FUNNEL		4	0	1.2	0	1.2	0	1
HOUSE TOP		12	0	1.2	0	1.2	0	3
INLET		0	0	0	0	0	0	1
OUTLET		10	0	1.2	0	0	0	1
RIBS		5	0	1.2	0	0	0	1
SOLID FLAP		8						
SOLID FUNNEL		4						
SOLID TEMP		1						
TEMP		1	0	1.2	0	1.2	0	1
RUBBER BOOT		5	0	1.1	0	0	0	1
WALL AFM AFTER		10	0	0	0	0	0	1
WALL AFM FLOW SIDE	YES	5	0.5	1.2	6	1.1	0	1
WALL BETWEEN RIBS		8	0	0	0	0	0	1
WALL FLAP BACK		5	0	1.1	0	1.2	0	1
WALL FLAP FRONT	YES	2	0.5	1.2	5	1.1	0	0.4
WALL FLAP SIDE	YES	2	0.5	1.2	4	1.1	0	0.4

Table 3.4 - The mesh parameters in case “B”

Part name	prism	max size	height	height ratio	num layers	tetra size ratio	tetra width	min size limit
AFM		5	0	1.1	0	1.2	0	1
FLAP		5	0	1.1	0	1.2	0	1
FLUID		15						
FUNNEL		4	0	1.2	0	1.2	0	1
HOUSE TOP		12	0	1.2	0	1.2	0	3
INLET		0	0	0	0	0	0	1
OUTLET		10	0	1.2	0	0	0	1
RIBS		5	0	1.2	0	0	0	1
SOLID FLAP		8						
SOLID FUNNEL		4						
SOLID TEMP		1						
TEMP		1	0	1.2	0	1.2	0	1
RUBBER BOOT		5	0	1.1	0	0	0	1
WALL AFM AFTER		10	0	0	0	0	0	1
WALL AFM FLOW SIDE	YES	5	0.4	1.2	5	1.1	0	1
WALL BETWEEN RIBS		8	0	0	0	0	0	1
WALL FLAP BACK		5	0	1.1	0	1.2	0	1
WALL FLAP FRONT	YES	2	0.4	1.2	3	1.1	0	0.4
WALL FLAP SIDE	YES	0.8	0.3	1.2	3	1.1	0	0.3

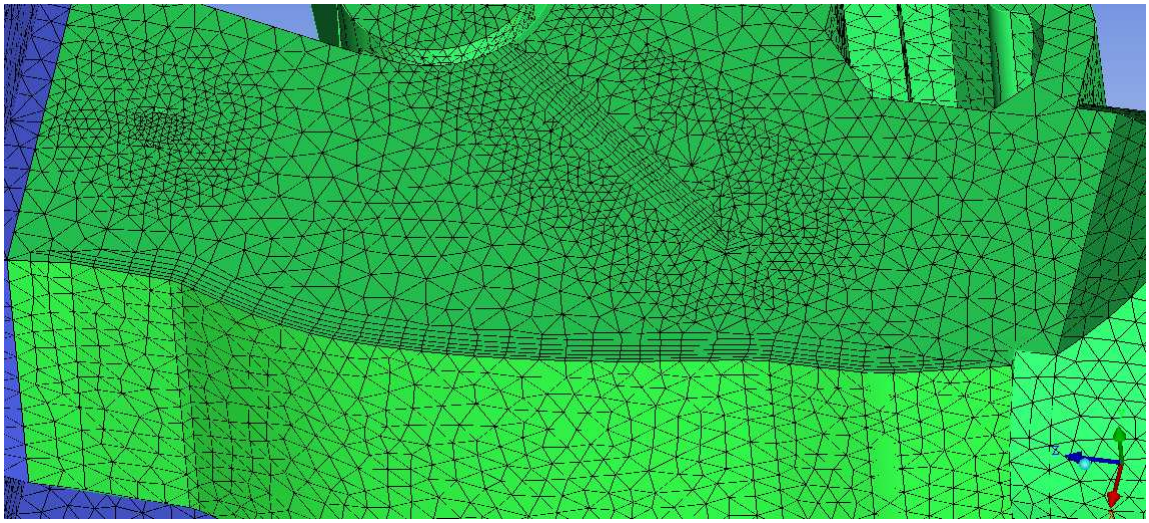

Figure 3.1 – Case “C” AFM mesh

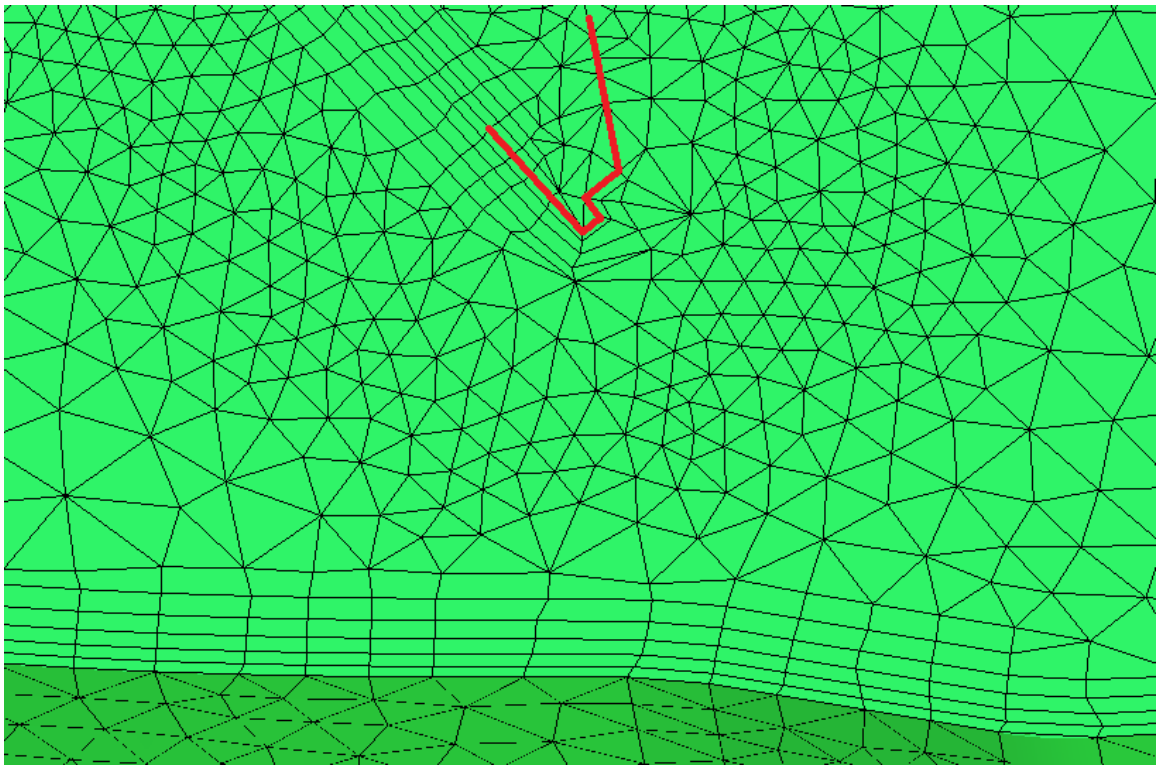

Figure 3.2 – Case “C” AFM mesh – gap (the contour of the flap is marked with red lines)

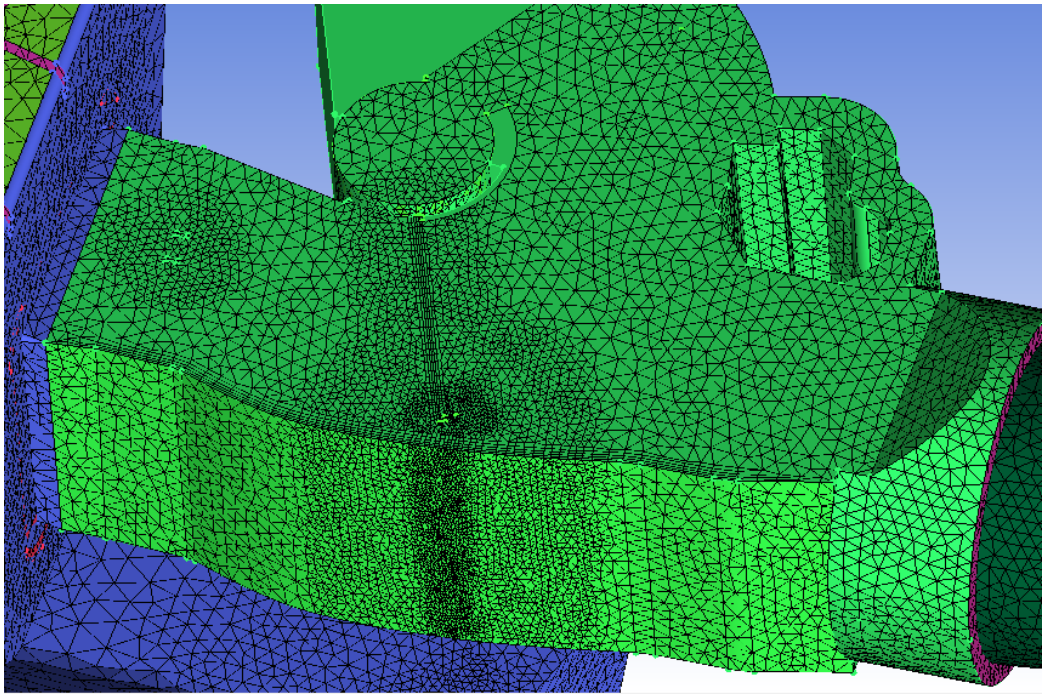

Figure 3.3 – Case “B” AFM mesh

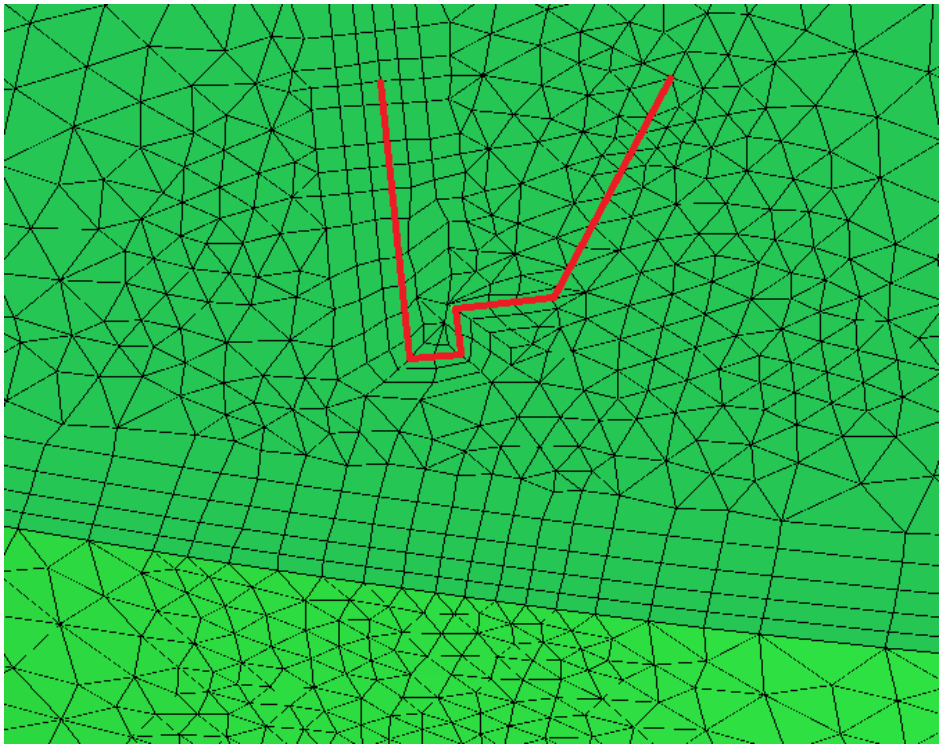

Figure 3.4 – Case “B” AFM mesh – gap (the contour of the flap is marked with red lines)

Remark: The current meshes contain the solid bodies (flap, temperature sensor, funnel), these solid body meshes will be removed for further investigations.

4 PREPARING THE SIMULATION

4.1 Simulation set-up

The simulation settings in FLUENT were the following.

Solver:
Pressure-based
Velocity formulation: Absolute
Time: Steady

Viscous model: k-ω – SST (default parameters)

Schemes:
Pressure-velocity coupling: Coupled
Spatial discretizations
- Gradient: Least squares cell based
- Pressure: Second order
- Momentum: Second order upwinding
- Turbulent kinetic energy: Second order upwinding
- Specific dissipation rate: Second order upwinding

Solution controls Default

Density model: Constant

Air properties
The viscosity and the density of the air were changed – to have the same value that occurred during the measurement.

4.2 Boundary conditions

The boundary conditions are based on the measurement data. Based on the flap angle the proper mass flow rate can be given and different pressure values related to it.

The reality the engine sucks air through the system. So the inlet should be a pressure inlet and the outlet should be such a boundary condition that allows us to prescribe the mass flow rate. In Fluent the outlet vent with target mass flow rate can be used for this.

Some preliminary simulations were carried out with these boundary conditions and quite slow convergence was experienced.

Therefore a pair of other type boundary condition was applied to investigate the convergence behavior and the effect on the flow field. Since a uniform flow field is assumed over the filter, there is no need to prescribe such a boundary (e.g. pressure inlet) on the inlet with which the inlet velocity profile can develop automatically by the flow itself. So with the assumption a uniform mass flow rate can be prescribed and an outflow on the outlet.

With these boundary conditions the solution converges in much less iterations and the flow field was very similar to previous one. Therefore mass flow rate inlet and outflow for outlet were used during the simulations. A detailed boundary condition dependence investigation is planed to carry out in the Final Project.

In all case the turbulent inlet varibles were the following:

Turbulent intensity	1%
Turbulent length scale	0.001 [m]

The values of the inlet mass flow rate are shown in **Table 4.1.** The mass flow rate values from the measurement were different for the cases with same flap angle. In the “B” cases the mass flow rate is 40.189 [kg/h] with funnel and 40.167 [kg/h] without funnel (this is 0.055% less). In the “C” cases the difference is larger, the mass flow rate is 160.438 [kg/h] with funnel and 159.464 [kg/h] without funnel (this is 0.607% less).

Table 4.1

Case	Mass flow rate ($\dot{m}$) [kg/s]
B0	0.0111574
B1	0.0111636
C0	0.0442955
C1	0.0445661

5 RESULTS

5.1 Pressure differences

During the measurement the wall static pressures to the ambient were measured with collector lines at 4 cross sections, 3 of them are located in the present simulation domain.

- Downstream of the filter (p_2)
- At the inlet cross section of the AFM (p_3)
- At the outlet cross section of the AFM (p_4)

The measurement and the simulation can be compared to each other if we take the difference of static pressure between the filter and different cross section values.

Table 5.1

	AFM inlet [Pa] p_3-p_2		AFM outlet [Pa] p_4-p_2		AFM pressure drop [Pa] p_4-p_3	
Case	Measurement	Simulation	Measurement	Simulation	Measurement	Simulation
B0	-22.40	-16.20	-832.66	-1379.43	-810.26	-1363.24
B1	-9.47	-11.05	-830.37	-1367.12	-820.90	-1356.07
C0	-373.59	-256.07	-1393.54	-1339.67	-1019.95	-1083.59
C1	-152.40	-173.94	-1343.04	-1314.20	-1190.64	-1140.26

The datasets from the measurements and from the simulations are collected in **Table 5.1**.

In case of the measurement at each cross section 4 pressure taps were applied and they were connectect to each other to have an average value.

In case of the simulation area weighted averages were calculated at the given cross sections.

In the “C” cases the values fit together quite well (only the inlet static pressure of the AFM has significant difference in the “C0” case).

In the “B” cases the inlet pressures are almost the same, but the pressure values at the AFM outlet are very different. The reason of this will be investigated in the future.

5.2 Flow fields with and without funnel

The difference of the flow fields between the cases with and without funnel is visualized with sectional streamlines.

Comparing **Figure 5.1** and **Figure 5.2** to each other a significant pressure distribution difference can be detected in front of the flap.

Comparing **Figure 5.3** and **Figure 5.4** to each other the separation at the inlet of the AFM can be seen if the funnel is not present, and one can notice that the z-velocity component upstream of the flap is more uniform in the “C1” case.

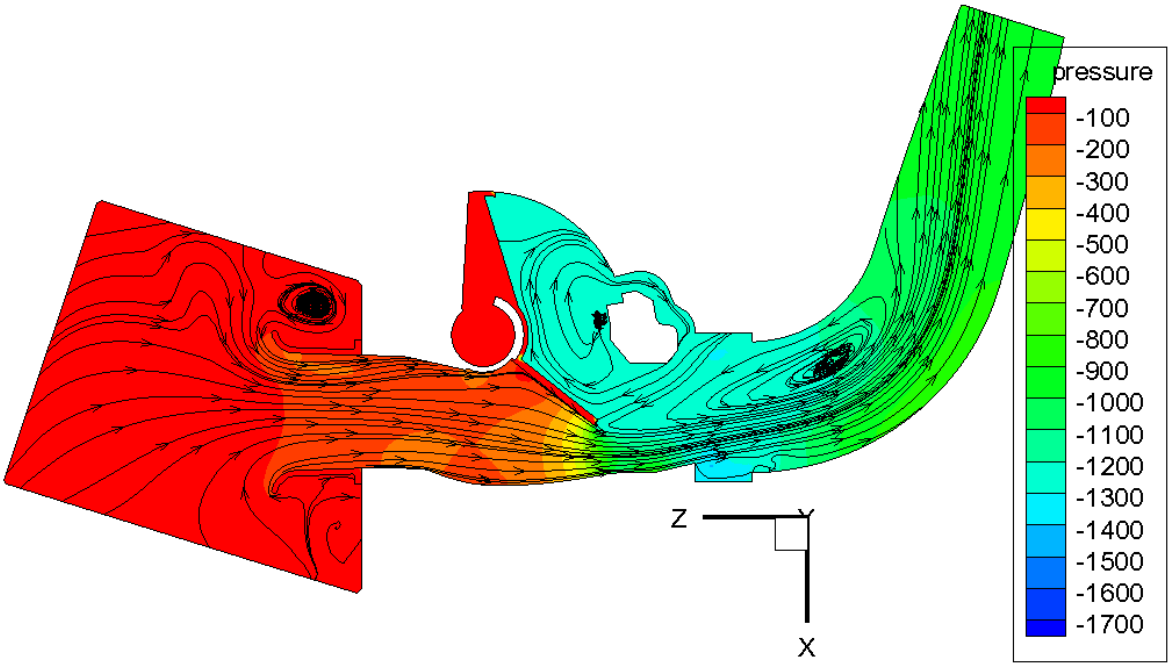

Figure 5.1 – Case “C1” – y-mid-plane sectional streamlines with pressure contour

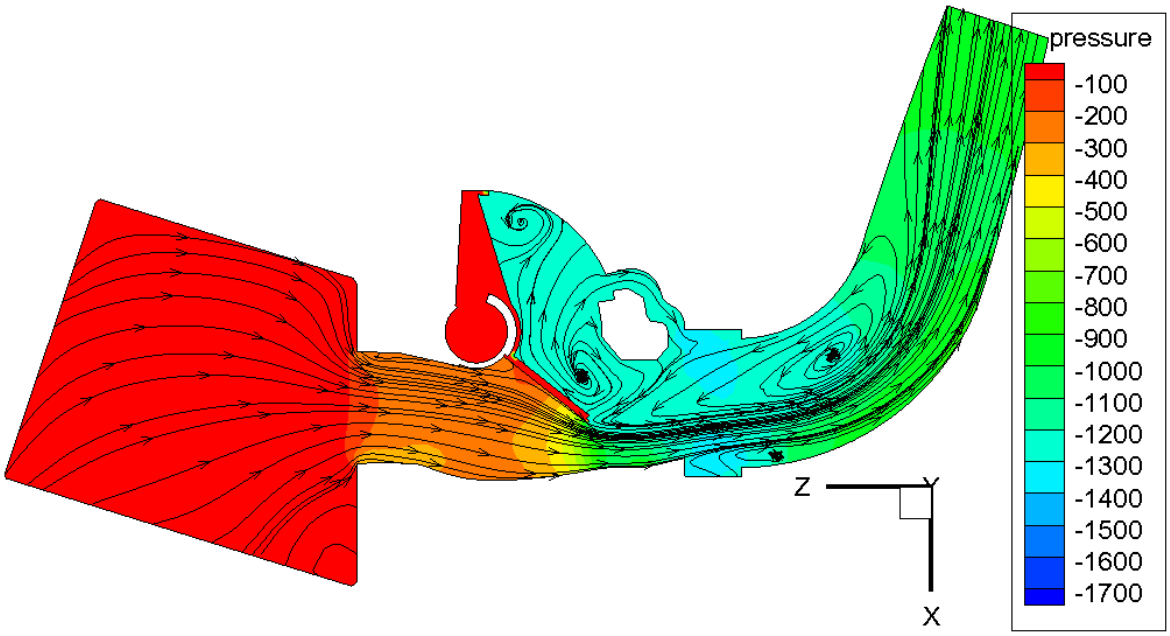

Figure 5.2 – Case “C0” – y-mid-plane sectional streamlines with pressure contour

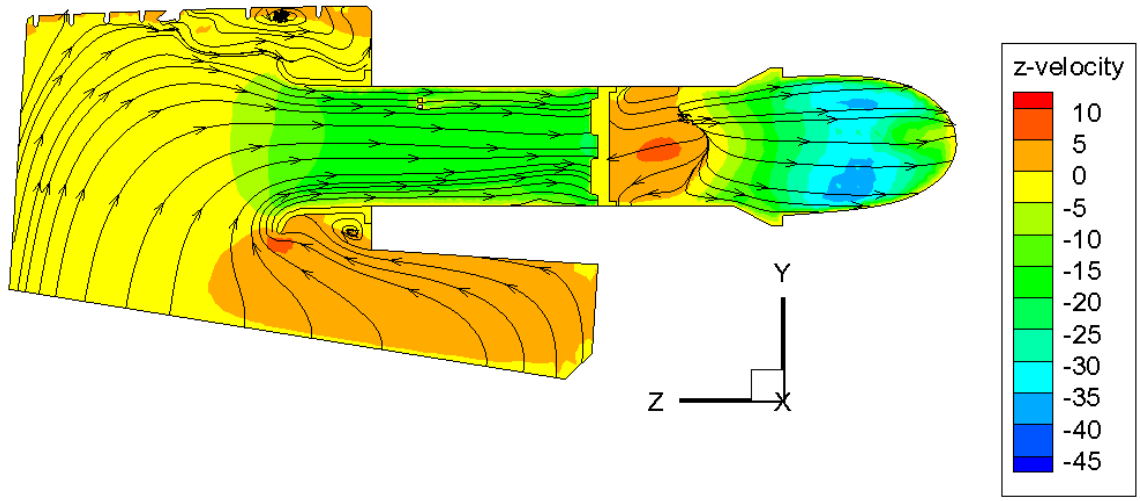

Figure 5.3 – Case “C1” – x-mid-plane sectional streamlines with velocity contour

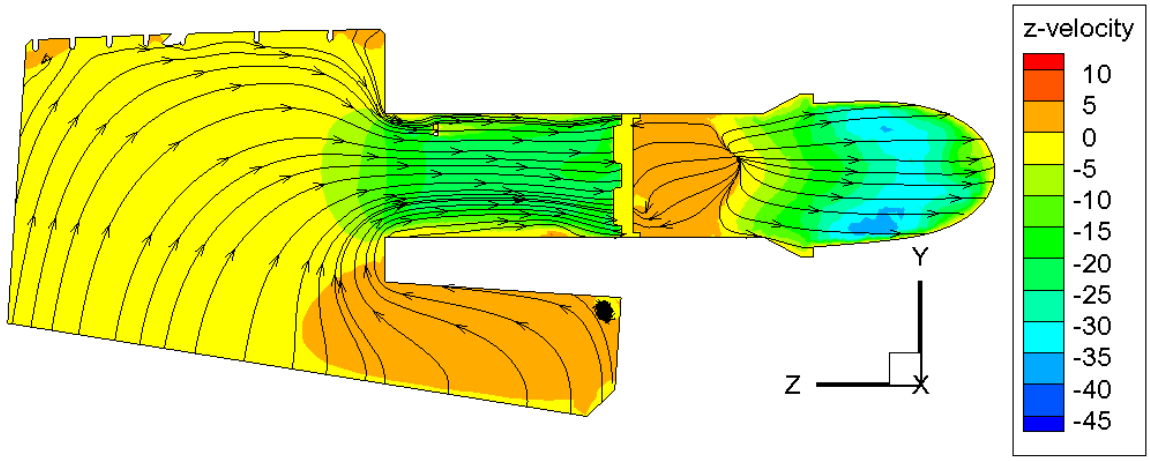

Figure 5.4 – Case “C0” – x-mid-plane sectional streamlines with velocity contour

The same conclusions can be stated if we compare the results of the “B0” and “B1” cases to each other.

5.3 Upstream vortices in the AFM

By investigating the secondary flow in the AFM some significant vortices can be detected in both cases when the funnel is present. On **Figure 5.5** some vortices can be seen and they are not present whithout funnel (**Figure 5.6**).

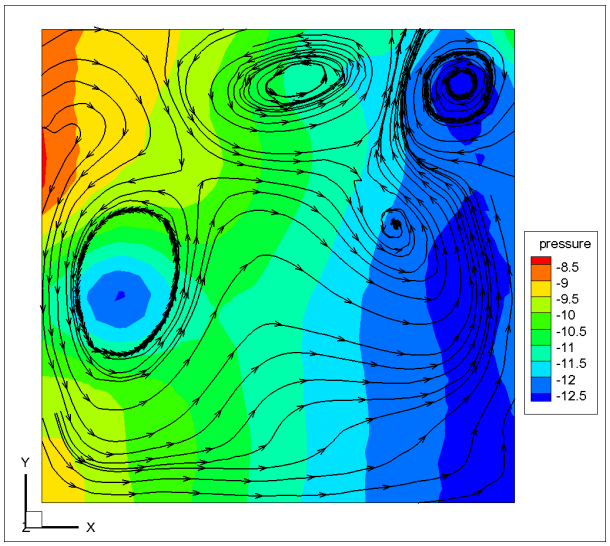

Figure 5.5 – Case “B1” – AFM inlet pressure distribution with sectional streamlines

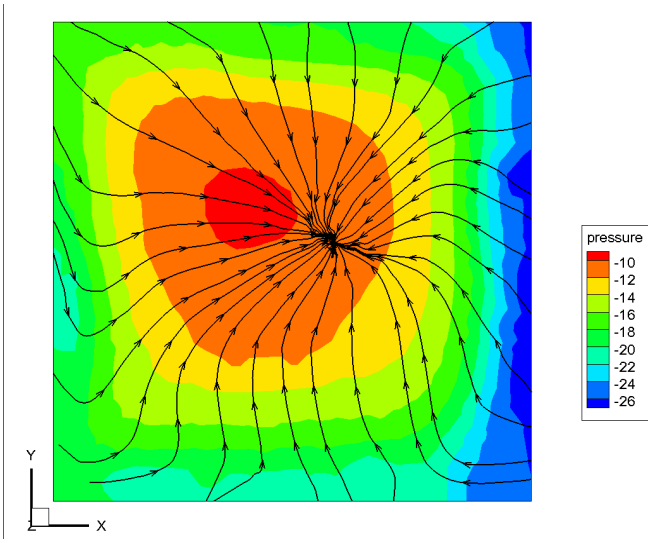

Figure 5.6 – Case “B0” – AFM inlet pressure distribution with sectional streamlines

6 FURTHER PLANS

The work on this project will continue during the next semester (2011/2012/I.) in course of Final Project.

Since in course of the Major Project the geometry modeling was the major task, the following further tasks of numerical simulation and result assessment side are defined.

- Checking the assumptions that lead to simulate only the upper part of the geometry (over the filter) and carrying out some simulations which include the filter.
- Detailed mesh dependency investigation to keep the cell number as low as possible.
- Detailed solver dependency investigation by changing the viscous model and the schemes and the density model of the fluid.
- Investigating the effect of the filter (check of homogeneity assumptions)
- Creating an optimized funnel, to improve to flow field before the AFM
- Investigating the effect of the temperature sensor on the flow field, force or moment on the flap.
- Investigating the effect of the ribs (wall roughness elements in filter housing).
- FSI with included damping chamber (only an idea, if the time allows it).

SUMMARY

In this project the effect of the presence of a funnel on the upstream flow conditions of an air flow meter (AFM) – which is used in a passenger car – were investigated by numerical simulations. Depending on the flow field (which depends on the presence of the funnel) the same flap angle can correspond to different mass flow rate values with or without funnel. This is crucial since the amount of air which is drawn by the engine is one of the most important input parameter of the ECU.
The main parts of the air intake system were modelled in 3D with SolidWorks. The important geometry features were kept, the unimportant ones – such as the outer surface details – were neglected during the geometry reconstruction.
Meshes were generated for six different cases (three flap angle position with and without funnel). Only part of the inner volume of the full model was meshed, because a quite uniform velocity distribution over the filter was assumed. The boundary conditions of the simulation based on measurements – carried out by Marcell BORIÁN.
The measurements showed that the case with small flap angle does not occur in real operation (even at idle engine operation the flap angle is higher), therefore four cases were simulated.
The k-ω – SST turbulence model was used with default parameters. The air density was considered as constant.
The static pressure results of the measurement and the simulation were compared by taking the difference of different cross sectional values. Using this method three values were compared in each case (inlet of the AFM, outlet of the AFM and the pressure drop).
One of the two different flap angle cases gave similar results, but the difference of the other results were significant at the outflow of the AFM.
The resulting flow fields showed significant difference in the topology of the flow upstream the flap. In cases when the funnel is present some large vortices could be identified upstream of the flap in the AFM. These vortices were not present in the cases without funnel.
Further investigations are planned to be carried out in Final Project.

BIBLIOGRAPHY

[1] Bosch Technical Instruction – L-Jetronic (1981, Robert Bosch GmbH, Automitive Equipment Division, Department for Technical Publications KH/VDT)

[2] BMW parts center webcatalogue (factory guide)

http://www.realoem.com/bmw/partgrp.do?model=AF91&mospid=47256&hg=13&fg=20
http://www.realoem.com/bmw/partgrp.do?model=AF91&mospid=47256&hg=13&fg=15

[3] BMW TechInfo – Technical Information System webcatalogue (factory guide)
http://www.bmwtechinfo.com/repair/main/561en/index.htm

[4] LAJOS Tamás: Az áramlástan alapjai (Műegyetemi Kiadó 2004, 3. kiadás)

[5] ANSYS User Guide (SAS IP, Inc., 2009)

APPENDIX

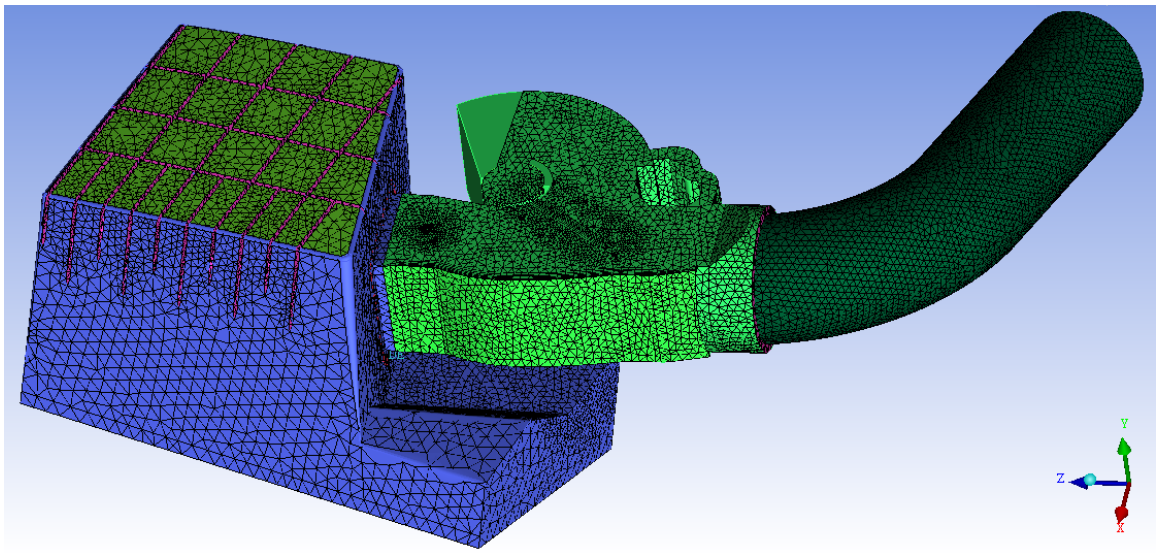

Figure A.1 – Full mesh – “C” case

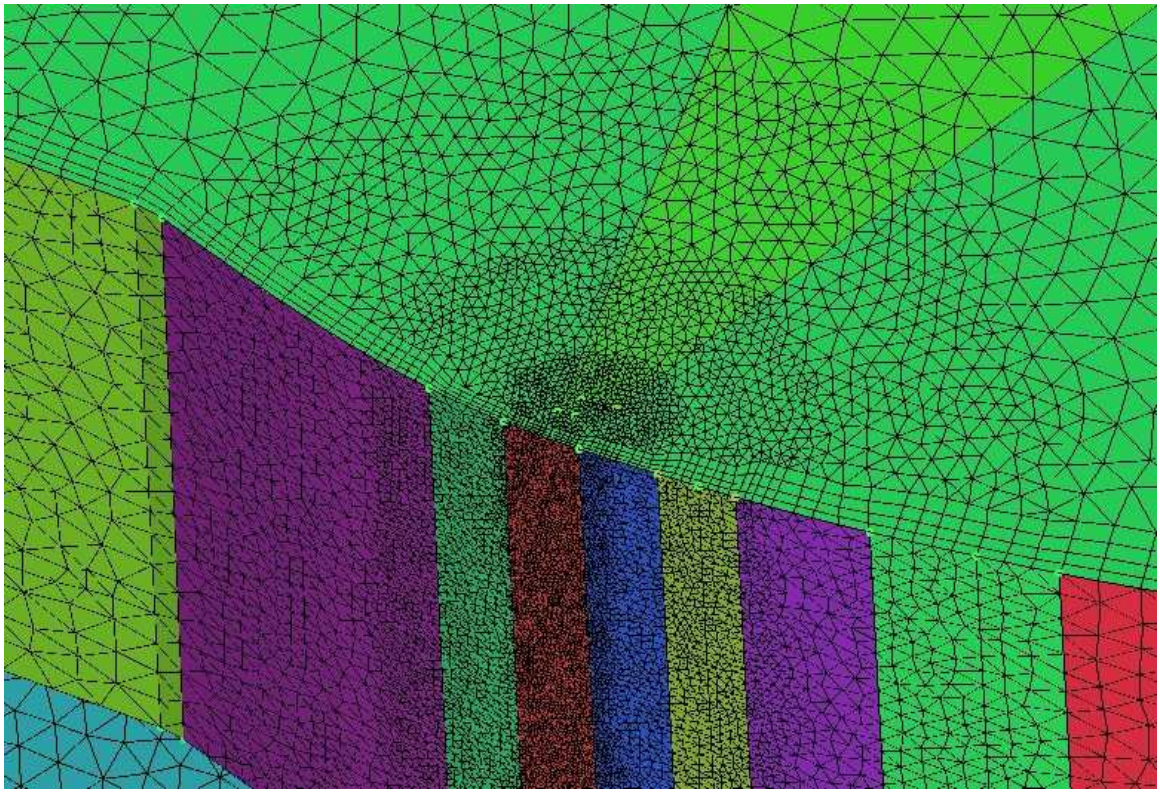

Figure A.2 – Gap region 1 – “A” case

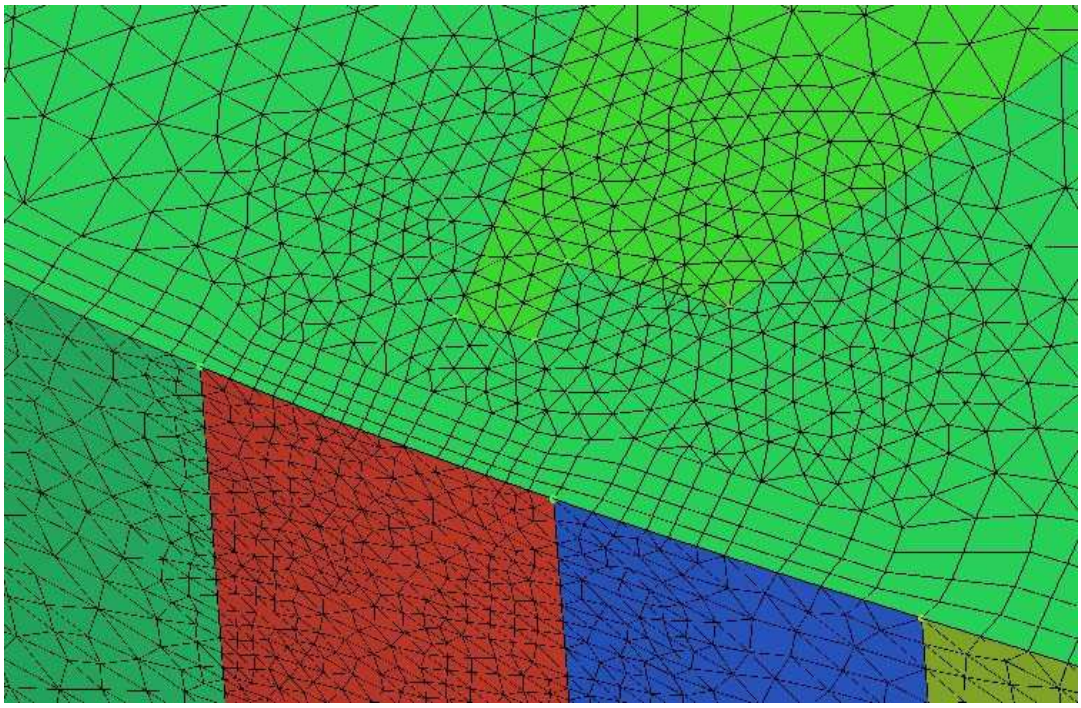

Figure A.3 – Gap region 1 – “A” case

Figure A.4 – The system in the car

Figure A.5 – Rubber boot

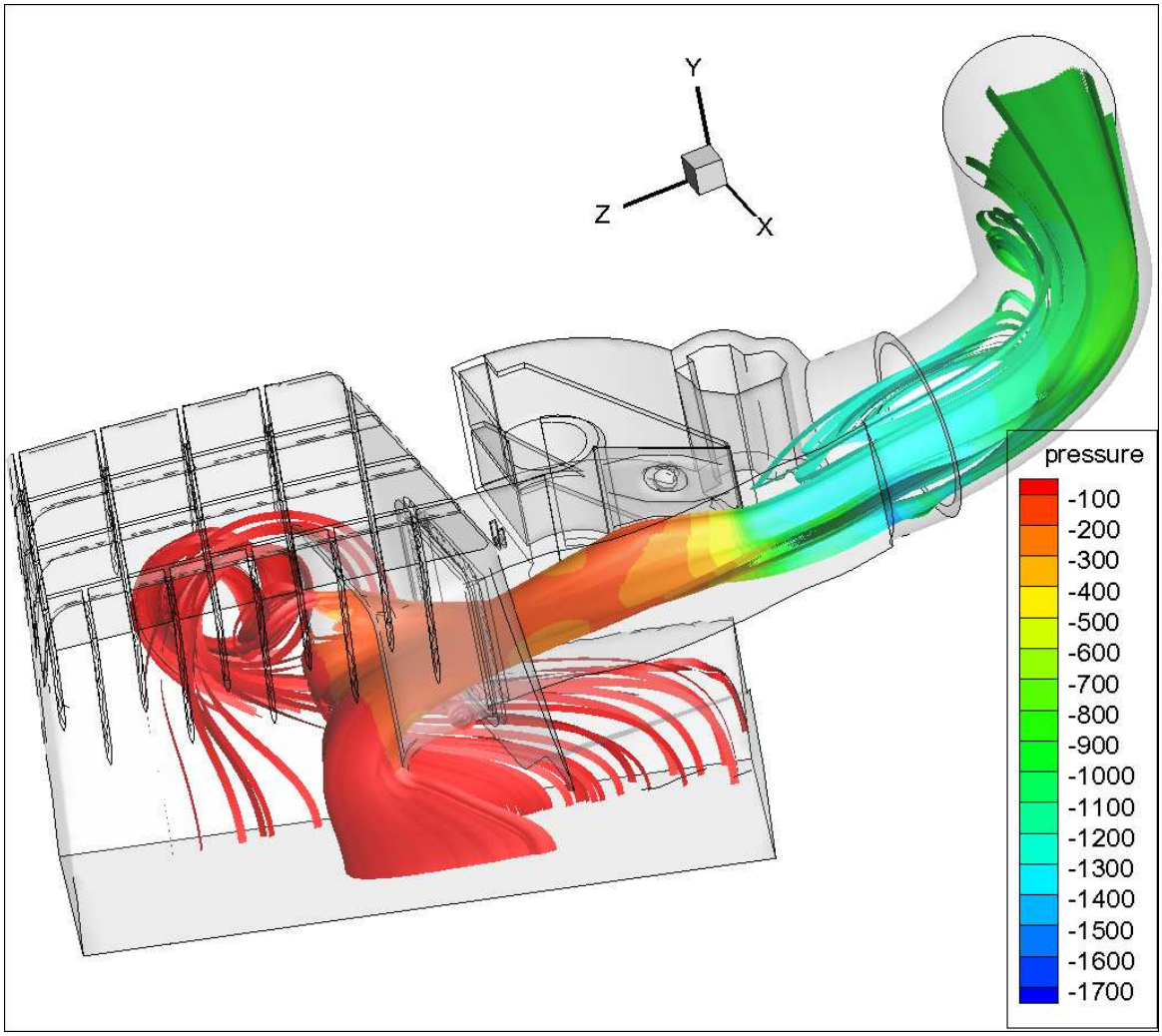

Figure A.6 – “C1” case stream visualization

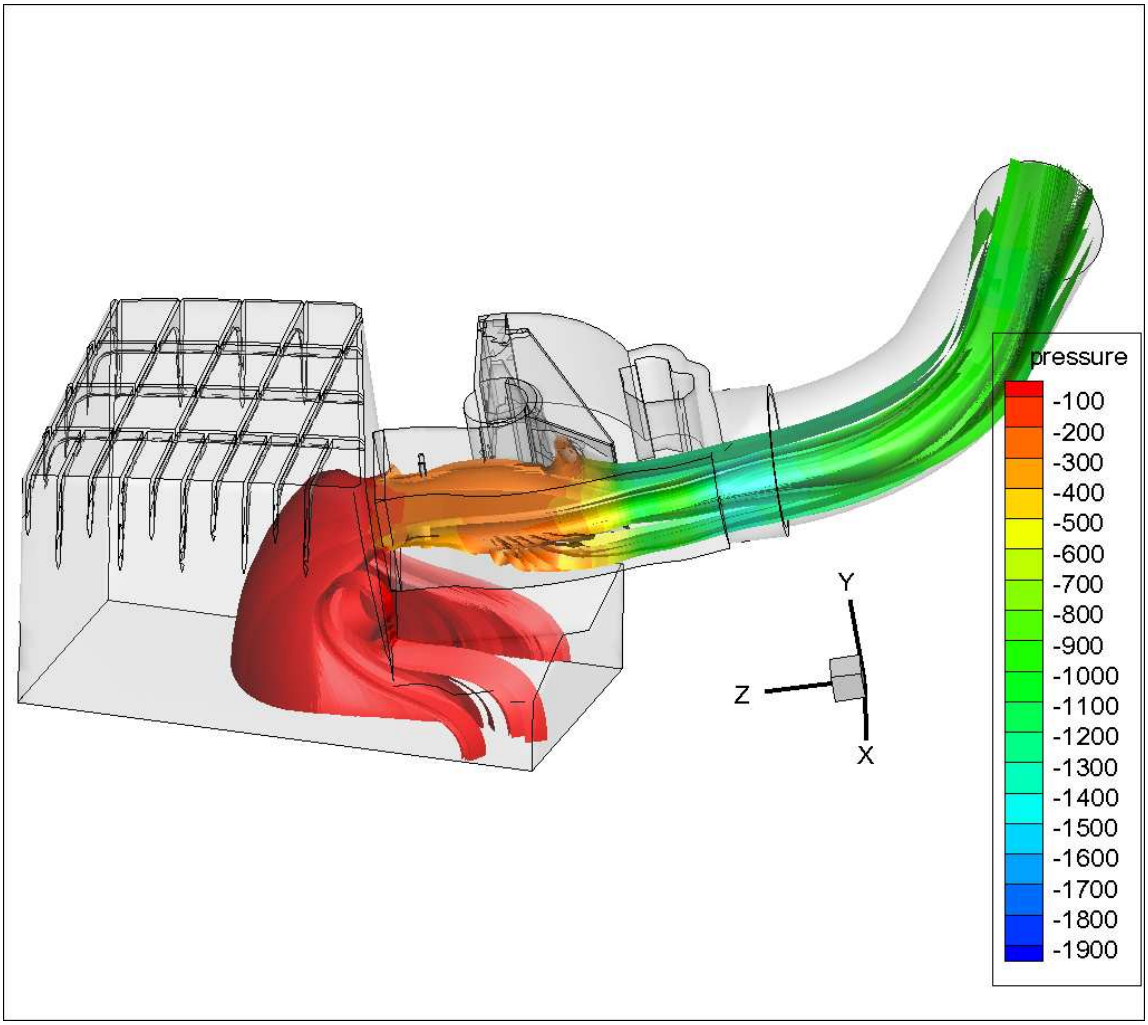

Figure A.7 – “C0” case stream visualization

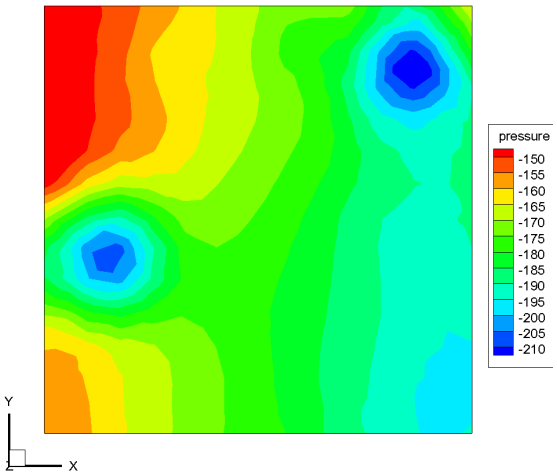

Figure A.8 – “C1” case AFM inlet pressure distribution

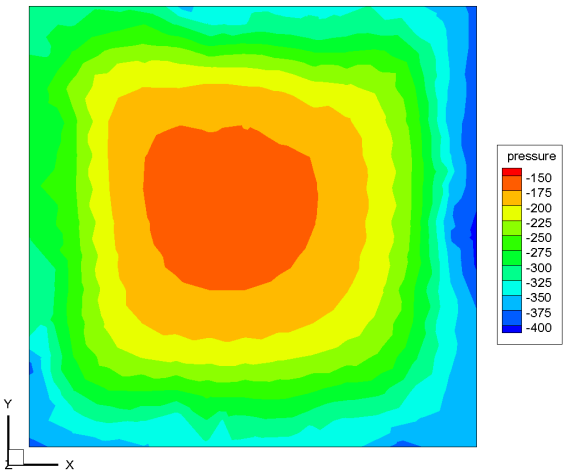

Figure A.9 – “C0” case AFM inlet pressure distribution

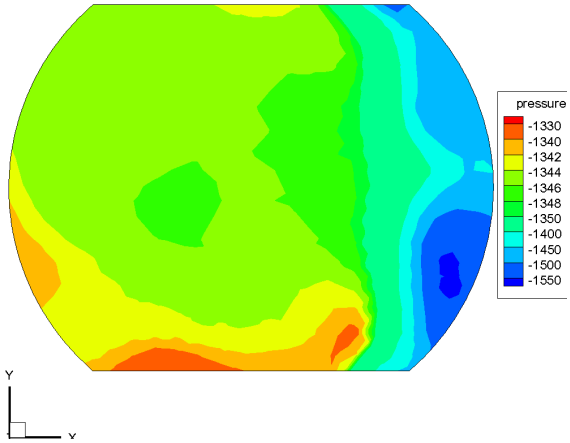

Figure A.10 – “B1” case AFM outlet pressure distribution

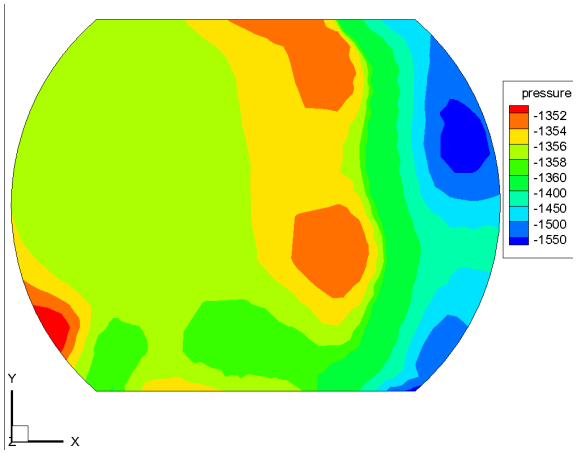

Figure A.11 – “B0” case AFM outlet pressure distribution

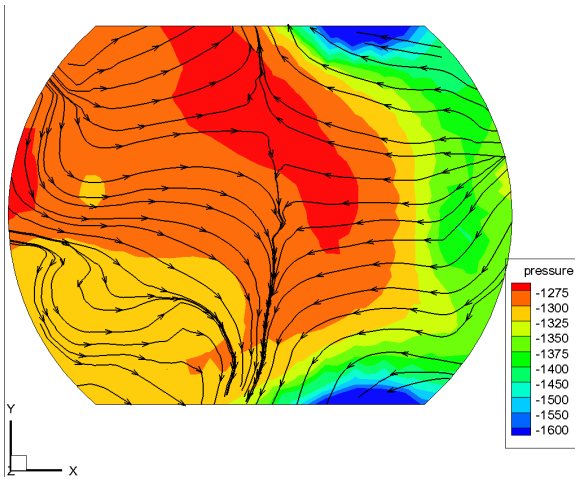

Figure A.12 – “C1” case AFM outlet pressure distribution with sectional streamlines

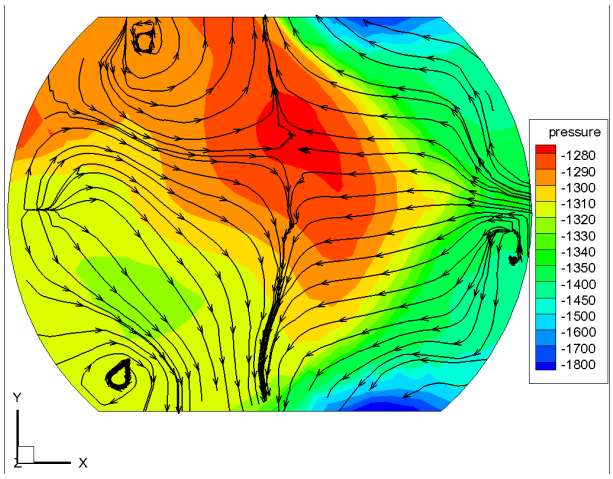

Figure A.13 – “C0” case AFM outlet pressure distribution with sectional streamlines